

The Mn-Ni (Manganese-Nickel) System

By N.A. Gokcen
Albany, OR

Equilibrium Diagram

The equilibrium phases of the condensed Mn-Ni system at 0.1 MPa (~1 atm) hydrostatic pressure are: (1) the liquid, L, above 1020 °C; (2) the bcc (δ Mn) terminal solid solution, with less than 6 at.% Ni; (3) the cubic (β Mn) terminal solid solution, containing less than 18 at.% Ni; (4) the cubic (α Mn) terminal solid solution, containing less than 9 at.% Ni; (5) the fcc (γ Mn,Ni) continuous solid solution, extending from 0 to 100 at.% Ni; (6) the ϵ phase (or Mn₂Ni), which has not yet been characterized; (7) the cubic, CsCl-type η phase, or ordered solid solution, MnNi(H), the high-temperature form of MnNi in the vicinity of the equiatomic composition; (8) the ordered fct AuCu-type η' phase, or MnNi(M); (9) the tetragonal η'' phase, or MnNi(Lo), not yet completely characterized, with $c/a = 0.94$ at 49 at.% Ni; (10) the ζ phase, or MnNi₂(H), not yet characterized; (11) the ζ' phase, or MnNi₂(Lo), not yet characterized; (12) the ordered fcc γ' phase with a Curie temperature of 520 °C, coincident with the peritectoid temperature; and (13) the ϕ phase (or Mn₃Ni), not yet characterized. The phase notation was adopted as a compromise from [69Tsi], [Hultgren,B], and [86Gup], with additional stoichiometric notation, such as MnNi(H, M or Lo) from [Hansen] and [69Tsi].

The assessed Mn-Ni diagram is shown in Fig. 1, and the associated invariant equilibria are listed in Table 1. The phase equi-

libria above 800 °C were fairly well established prior to 1968, but below this temperature and after 1969, most of the diagram is from [69Tsi]. Figure 1 is based largely on the results of [32Dou], [48Kos], [49Kur], [51Col], [52Ere1], [52Ere2], [57Hel], [58Hah], and [69Tsi]. Minor inconsistencies between the phase diagram and the text both in [69Tsi] are resolved in the present paper.

The data compiled in [Hansen], [Elliott], and [Shunk] below 800 °C are inadequate, and the estimated phase boundaries are incorrect except above 1000 °C, and at 40 to 50 at.% Ni above 670 °C. The extensive and systematic investigation with 48 alloys between 1.7 to 95.4 at.% Ni by [69Tsi] supersedes nearly all the data below 800 °C and less than 80 at.% Ni.

Liquidus and Solidus

Earlier results of [32Dou], [48Kos], [49Kur], [52Ere1], and [52Ere2] agree well with the careful work of [51Col] in the range 10 to 100 at.% Ni. The portion from 0 to 10 at.% Ni and the peritectic area were established accurately only by [57Hel] using thermal analysis. The results of [51Col] and [57Hel] are adopted here in preference to other data, with a correction of 2 °C for converting their 1948-IPTS temperatures to 1968-IPTS temperatures. The minimum in both curves occurs at 38 at.% Ni and 1020 °C from [51Col], in very close agreement with [49Kur] and [52Ere1] and the values adopted by [69Tsi].

Table 1 Special Points of the Assessed Mn-Ni Phase Diagram

Reaction	Composition of the respective phases, at.% Ni			Temperature, °C	Reaction type
L ↔ Ni		100		1455	Melting
L ↔ δ Mn		0		1246	Melting
δ Mn + L ↔ (γ Mn,Ni)	6	10	7	1164	Peritectic
δ Mn ↔ γ Mn		0		1138	Allotropic
γ Mn ↔ β Mn		0		1100	Allotropic
L ↔ (γ Mn,Ni)		38		1020	Congruent
(γ Mn,Ni) ↔ η		49		911	Congruent
η + (γ Mn,Ni) ↔ η'	52	57	55.5	775	Peritectoid
β Mn ↔ α Mn		0		727	Allotropic
(γ Mn,Ni) ↔ ϵ		33.7		720	Congruent
(γ Mn,Ni) ↔ ζ		66.6		710	Congruent
η ↔ (γ Mn,Ni) + η'	45	40	47	675	Eutectoid
(γ Mn,Ni) ↔ η' + ζ	61	53	64	655	Eutectoid
(γ Mn,Ni) ↔ ϵ + η'	38	35.5	47	640	Eutectoid
η' ↔ ϵ + ζ	48	35	66	620	Eutectoid
(γ Mn,Ni) ↔ (β Mn) + ϵ	29	18	31.5	615	Eutectoid
(β Mn) ↔ (α Mn) + ϵ	16	9	32.5	586	Eutectoid
ζ ↔ ϵ + (γ Mn,Ni)	68.5	34	73.5	580	Eutectoid
ϵ ↔ (α Mn) + (γ Mn,Ni)	34	7.5	74	560	Eutectoid
(α Mn) + (γ Mn,Ni) ↔ γ'	5	75	73	520	Peritectoid
(α Mn) + γ' ↔ η''	2.7	71	48.5	480	Peritectoid
η'' + γ' ↔ ζ'	50	73	66.7	440	Peritectoid
(α Mn) + η'' ↔ ϕ	1.5	46.5	25	430	Peritectoid

Section II: Phase Diagram Evaluations

Mn-Rich Solid Phases

The boundaries of δ phase were determined by [57Hel]. The $(\beta\text{Mn}) + (\delta\text{Mn,Ni})$ two-phase boundaries of [48Kos] are too wide, and those of [49Kur] and [51Col] are too narrow. Closer agreement exists between [52Ere1] and [52Ere2] and [69Tsi] at 850 to 1100 °C. The $(\delta\text{Mn},\gamma\text{Mn,Ni})$ side of the boundaries agrees

approximately in all the preceding investigations. The results of [69Tsi] are adopted in Fig. 1. The only set of reliable data for the (αMn) phase boundaries are from [69Tsi].

The $(\gamma\text{Mn,Ni})$ phase boundaries are from [51Col] and [57Hel] above 800 °C and beyond 20 at.% Ni; however, below that temperature and 0 to 100 at.% Ni, the boundaries from [69Tsi] are

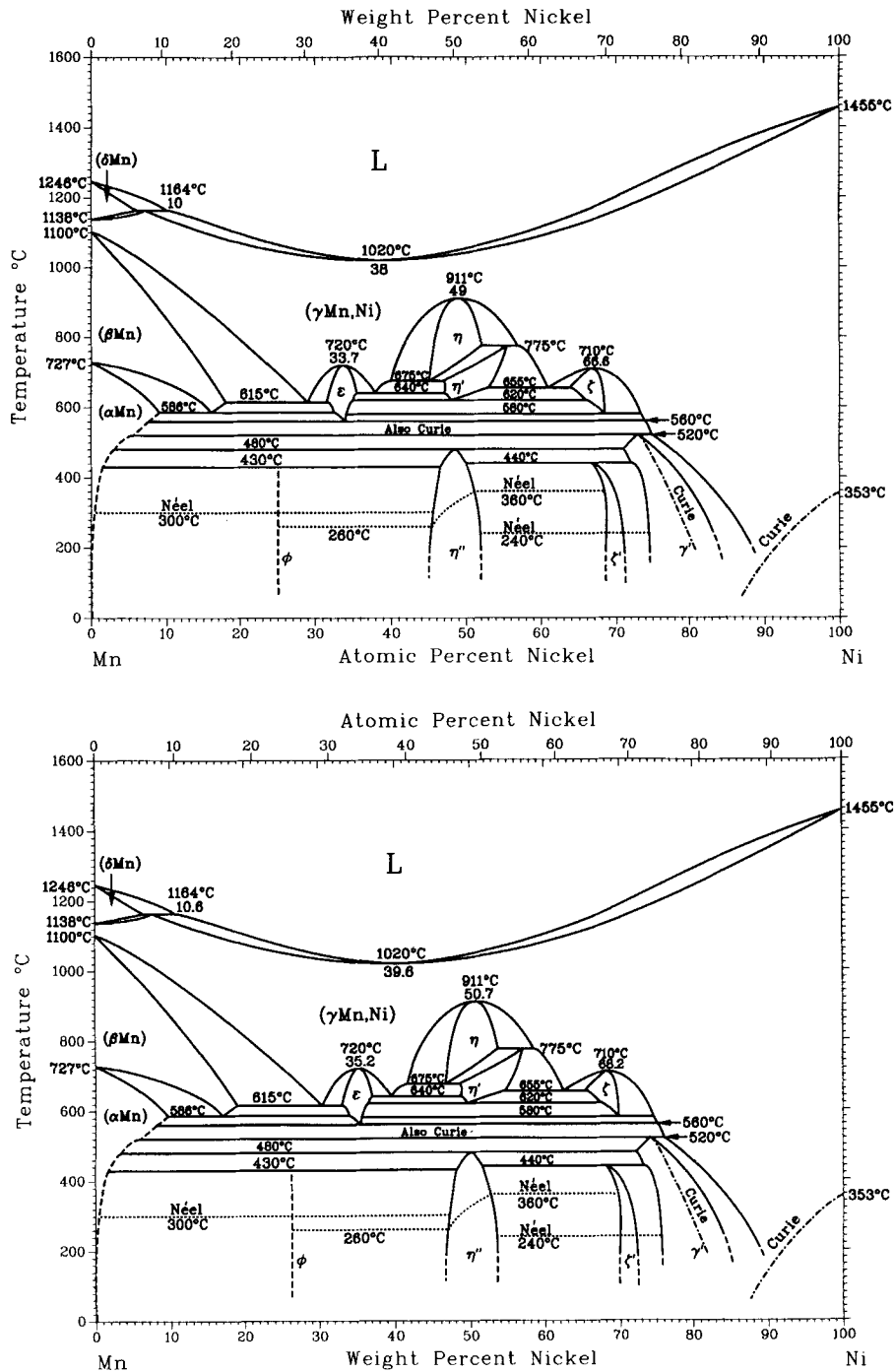


Fig. 1 Assessed Mn-Ni phase diagram.

adopted. Both pure γ Mn and Ni are fcc, and the entire (γ Mn,Ni) region is also fcc.

η or MnNi(H)

The phase boundaries of η , the ordered cubic CsCl-type phase from 780 to 911 °C, are from the careful microscopic and X-ray data of [51Col]. Below 780 °C, the entire region is taken from the extensive and careful work of [69Tsi], with long anneals, differential thermal analysis (DTA), magnetic analysis, X-ray diffraction (XRD), and light and electron microscopy. Selected areas of this region are in excellent agreement with [51Col], i.e., the eutectoid temperature of 675 °C and the phase boundaries above this temperature at compositions below 50 at.% Ni. The maximum point of 49 at.% Ni and 911 °C is from [51Col], with a small temperature scale correction. This phase cannot be retained by quenching to ambient temperature, because it transforms into martensitic ordered η' phase.

Remaining Phases and Their Boundaries

The remaining phase boundaries were determined accurately by [69Tsi]. Above 520 °C, most of the data were obtained by DTA with a slow heating rate of 3 °C/min. The peritectic temperature of 520 °C coincides with the Curie temperature, as determined by DTA and magnetometry. The remaining phase boundaries were also determined by DTA, except as follows. The (γ Mn,Ni)/(γ Mn,Ni) + γ' boundary was determined by magnetometric measurements below 400 °C, which complement the magnetic measurements of [58Hah] above 400 °C.

The (γ Mn,Ni)/ γ' phase boundary beyond 75 at.% Ni was considered for a long time [Hansen] to be a second-order phase boundary—the transformation of a disordered fcc phase, (γ Mn,Ni), into an ordered fcc phase, γ' , in the vicinity of MnNi₃ on cooling. However, the transformation is by nucleation and growth [61Mar, 63Kro], and it is interpreted to be a first-order transformation [61Mar, 69Tsi, 74Bee, 77Koz]. Reports of the existence of

Table 2 Mn-Ni Crystal Structure Data

Phase	Composition, at. % Ni	Pearson symbol	Space group	Strukturbericht designation	Prototype	Reference
(δ Mn)	0 to 6	<i>cI2</i>	<i>Im$\bar{3}m$</i>	A2	W	[Pearson3]
(γ Mn,Ni)	0 to 100	<i>cF4</i>	<i>Fm$\bar{3}m$</i>	A1	Cu	[Pearson3]
(β Mn)	0 to 18	<i>cP20</i>	<i>P4₁32</i>	A13	β Mn	[Pearson3]
(α Mn)	0 to 9	<i>cI58</i>	<i>I$\bar{4}3m$</i>	A12	α Mn	[Pearson3]
η (a)	45 to 52	<i>cP2</i>	<i>Pm$\bar{3}m$</i>	B2	CsCl	[68Kre]
η'	47 to 55.5	<i>tP4</i>	<i>P4/mmm</i>	L10	AuCu	[Pearson3]
γ'	71 to 85	<i>cP4</i>	<i>Pm$\bar{3}m$</i>	L12	AuCu ₃	[Pearson3]

(a) At 745 °C; this phase cannot be retained by quenching.

Table 3 Mn-Ni Lattice Parameter Data at Room Temperature

Phase	Composition, at. % Ni	Lattice parameters, nm		Comment	Reference
		<i>a</i>	<i>c</i>		
δ Mn	0	0.30813	...	At 1137 °C(a)	[90Gok]
γ Mn	0	0.38626	...	At 1097 °C(a)	[90Gok]
β Mn	0	0.63151	...	(a)	[90Gok]
α Mn	0	0.89139	...	(a)	[90Gok]
(β Mn)	5	0.63384	[Pearson1]
	10	0.63553	[Pearson1]
	15	0.63696	[Pearson1]
(γ Mn,Ni)	20	0.37025	[65Pat]
	30	0.36970	[Pearson1]
	40	0.36860	[Pearson1]
	50	0.36660	[85Ada]
	60	0.36334	[Pearson1]
	80	0.35788	[Pearson1]
	90	0.35530	[Pearson1]
	95	0.35380	[Pearson1]
η	47.7	0.3749	...	At 935 °C	[51Col]
	51.9	0.374	...	At 935 °C	[51Gol]
	50	0.2977	...	At 750 °C	[51Col,68Kre]
η'	46	0.3734	0.3645	...	[85Ada]
	50	0.3731	0.3632	...	[85Ada]
	52	0.3729	0.3625	...	[85Ada]
γ'	75	0.3589	[61Mar]
Ni	100	0.35240	[Massalski]

(a) Variation of *a* with temperature given in [90Gok].

Section II: Phase Diagram Evaluations

ϕ are based only on magnetometric measurements, coupled with the peritectoid temperature determination of [69Tsi] by DTA at 430 °C. Electrolytic Mn of 99.9 at.% purity and carbonyl Ni of even greater purity became available after 1932. In nearly all the careful investigations cited after 1932, Mn and Ni of at least 99.9 at.% purity were used.

Curie and Néel Temperatures

The Curie temperature of 520 °C from [69Tsi], coincident with the peritectoid temperature, is in agreement with [58Hah] and [41Vol]. The Curie temperatures within the γ' phase were determined magnetically by [58Hah] and rechecked by [69Tsi]. The Curie temperatures from about 86 to 100 at.% Ni, measured by the magnetometry of [69Tsi], are preferred to the earlier and higher temperatures obtained by [Hansen] from their interpolation of the earlier data.

The Néel temperature of 300 °C for ϕ , that of 260 °C for η'' , increasing within η'' to 360 °C, and that of 240 °C for ζ' were determined by [69Tsi] with magnetometry. The ordered fcc γ' region is strongly ferromagnetic; MnNi₃ quenched from the temperatures above the (γ Mn,Ni)/(γ Mn,Ni) + γ' boundary is paramagnetic [31Kay, 40Tho, 41Vol, 55Shu, 58Hah].

ζ' is probably metamagnetic [69Tsi] (remnant, weakly magnetic). η'' and ϕ are antiferromagnetic [59Kas, 68Kre, 68Pal] (see also [68Hic], [69Tsi], and [83Ego]).

Metastable Phases

The structure of splat quenched alloys with Ni concentrations at 4.7 at.% intervals within 4.7 to 48.3 at.% Ni were investigated by [81Ogd] using small angle and ordinary X-ray scattering. The short-range order of atoms was described by an fcc lattice. Radial distribution of atoms was obtained, and it was shown that the lattice parameter first increases up to about 20 to 25 wt.% Ni and then decreases. Water quenching of samples from 927 °C and containing 11.3 to 28.6 at.% Ni yielded an acicular fct structure [65Pat], only suggesting possible martensite transformation.

The transformation of η into η' is martensitic of nearly thermoelastic nature, according to [85Ada]. Martensitic structure was observed in the alloys within the region with 50 at.% Ni or less after quenching. The martensite plates were internally twinned on {111} planes. Slow cooling from η and η + (γ Mn,Ni) regions with less than 50 at.% Ni became tempered and exhibited low-density twins crossing one another. Ni-rich quenched alloys showed a finely twinned structure different from martensite, with a twin plane of {101} due to ordering. The crystal structure of both Ni-rich and Ni-lean phases were the same $L1_0$ structure [85Ada]. Extensive micrographs and diffraction data were also presented by [85Ada] (see also [67Kra]).

Crystal Structures and Lattice Parameters

Mn-Ni crystal structure and lattice parameter data are summarized in Tables 2 and 3, respectively.

(α Mn) and (δ Mn)

The crystal structure of these terminal solid solutions are the same as the corresponding pure Mn phases. The lattice parameters are not known, but they are likely to be within $\pm 0.4\%$ of the parameters for the pure Mn phases at the highest solute concentrations, based on the data for similar alloys [Pearson1, Pearson2, Pearson3].

(β Mn)

The cubic A13 (β Mn) phase can be quenched to room temperature to retain its structure. Samples containing 0 to 14.6 at.% Ni were homogenized and then quenched to obtain powder samples for diffraction by [51Col]. The lattice spacing increases about 0.9% in this range, as shown in Table 3.

(γ Mn,Ni)

The fcc (γ Mn,Ni) alloy samples can be water quenched to retain this phase at ambient temperatures. For the mid-range compositions, iced-brine or cryogenic quenching is necessary [85Ada]. All the existing data are concordant [48Kos, 57Pea, 85Ada] (see also [Pearson1] and [Pearson3]). The data in Table 3 are taken to be the best available averaged set in this assessment.

ϕ

The crystal structure of this phase is not known. If it is assumed that the samples quenched from (γ Mn,Ni) with 25 at.% Ni could transform into ϕ , from the results of [65Pat], ϕ is fct with $a = 0.3698$ and $c = 0.3692$ nm. Clearly this is a speculation at this time, because no specific data exist.

ϵ

The structural data for this phase are not available.

η

This phase in the vicinity of MnNi is a fully ordered, CsCl structure, as first discovered through neutron diffraction by [68Kre]. The X-ray data of [51Col] for 47.7 at.% Ni at 745 °C and the neutron diffraction data of [68Kre] for 46.5 to 54.5 at.% Ni at 760 °C give a recommended value, $a = 0.2977$ nm at 750 °C. This phase was considered to be bcc, A2, until the use of neutron diffraction by [68Kre]. The interpretation in [Pearson1] and [Pearson3] is incorrect.

This phase transforms into another ordered phase, η' , irrespective of the quenching rate. The transformation is diffusionless and martensitic, and faster quenching yields η' with greater lattice distortions (see "Metastable Phases," above).

η'

This fully ordered, fct phase is of the AuCu type (often referred to as AuCuI type), with the $L1_0$ structure, as determined by X-ray and neutron diffraction [48Kos, 59Kas, 68Kre, 85Ada]. The data listed in Table 3 are from a linear plot in [85Ada] containing all the reliable data. The data of [85Ada] for 47 to 50 at.% Ni are for carefully homogenized samples quenched mostly in iced brine from 800 °C. The scatter in the diffraction data is probably due to the effect of quenching on the microstructure of η' . The X-ray data of [65Pea] do not agree with the foregoing data, but the data for one

Table 4 Thermodynamic Properties of Solid Mn-Ni Alloys
 $x\text{Mn}(\beta) + (1-x)\text{Ni}(\gamma) = \text{Mn}_x\text{Ni}_{1-x}$

Composition, atom fraction Ni	Phase	$\Delta_f G^{\text{ex}}$, J/mol	$G_{\text{Mn}}^{\text{ex}}$, J/mol	$G_{\text{Ni}}^{\text{ex}}$, J/mol
At 1050 K				
0.1	(βMn)	-4150	-1700	-26 180
0.13	(βMn)(a)	-5680	-2870	-24 460
0.21	($\gamma\text{Mn,Ni}$)(a)	-7610	-2020	-28 650
0.30	($\gamma\text{Mn,Ni}$)	-9640	-4130	-22 490
0.41	($\gamma\text{Mn,Ni}$)(b)	-11 110	-7720	-15 980
0.46	η (b)	-11 560	-6940	-16 980
0.52	η (c)	-11 620	-15 870	-7690
0.57	($\gamma\text{Mn,Ni}$)(c)	-11 250	-14 910	-8490
0.70	($\gamma\text{Mn,Ni}$)	-9640	-22 490	-4130
0.80	($\gamma\text{Mn,Ni}$)	-7350	-29 380	-1840
0.90	($\gamma\text{Mn,Ni}$)	-4130	-37 180	-460
1.0	($\gamma\text{Mn,Ni}$)	0	-45 900	0
At 1200 K				
0.073	(βMn)(d)	-3370	-1290	-29 780
0.125	($\gamma\text{Mn,Ni}$)(d)	-5020	-720	-35 140
0.20	($\gamma\text{Mn,Ni}$)	-7350	-1840	-29 380
0.30	($\gamma\text{Mn,Ni}$)	-9640	-4130	-22 490
0.40	($\gamma\text{Mn,Ni}$)	-11 010	-7340	-16 520
0.50	($\gamma\text{Mn,Ni}$)	-11 480	-11 480	-11 480
0.60	($\gamma\text{Mn,Ni}$)	-11 010	-16 520	-7340
0.70	($\gamma\text{Mn,Ni}$)	-9640	-22 490	-4130
0.80	($\gamma\text{Mn,Ni}$)	-7350	-29 380	-1840
0.90	($\gamma\text{Mn,Ni}$)	-4130	-37 180	-460
1.0	($\gamma\text{Mn,Ni}$)	0	-45 900	0

(a) (βMn) and ($\gamma\text{Mn,Ni}$) are coexisting in equilibrium. (b) ($\gamma\text{Mn,Ni}$) and η are coexisting in equilibrium. (c) η and ($\gamma\text{Mn,Ni}$) are coexisting in equilibrium. (d) (βMn) and ($\gamma\text{Mn,Ni}$) are coexisting in equilibrium.

composition in [Pearson3] are correct. The ordered η' is antiferromagnetic from 0 K to its Néel temperature [68Kre, 68Pal].

η''

This tetragonal phase at 48.5 at.% Ni with $c/a = 0.94$ [69Tsi] has not been characterized fully. A number of samples of 45 to 50 at.% Ni quenched from 800 °C were heated to 480 °C for 50 h by [85Ada]. At this temperature, which is the peritectoid temperature for η'' , these samples gave the same diffraction patterns as those for η' that were quenched from 800 °C. It appears, therefore, that η' and η'' might have the same diffraction data. (No reference was made by [85Ada] to [69Tsi]; therefore, no interpretation was made of η'' by [85Ada].)

ζ and ζ'

Structural data for these phases are not available. Based on similar phases listed in [Pearson1] and [Pearson2], it is likely that these phases are tetragonal.

γ'

This ordered fcc phase, with a wide range of composition about MnNi_3 has been investigated thoroughly, partly due to its strong ferromagnetism and partly because of the controversy prior to 1960 on the order of transition from ($\gamma\text{Mn,Ni}$) to γ' . Nearly perfectly ordered γ' can be obtained from ($\gamma\text{Mn,Ni}$) by long annealing

treatments. Special X-ray and neutron diffraction [49Shu, 55Shu, 61Mar, 65Sid, 66Pao, 67Pao, 68Pal, 77Koz] and Mössbauer spectroscopy [63Kro] were used to study ($\gamma\text{Mn,Ni}$) and γ' . The XRD data of [61Mar] for both ordered and disordered phases yielded $a = 0.3589$ nm. The temperature dependence of the degree of long-range order in the ordered phase was established by [77Koz] using the monochromatized FeK_α radiation (see also [67Pao] for a different technique).

Thermodynamics

Solid Phases

Thermodynamic properties of Mn-Ni solid phases were investigated by Knudsen effusion cell vapor pressure measurement [62Poz] at 916 to 963 °C, the galvanic cell method with a liquid electrolyte [68Ere] at 677 to 877 °C, and with $\text{ThO}_2\text{-Y}_2\text{O}_3$ and with CaF_2 solid electrolytes at 677 to 1075 °C [83Ven]. All the investigations cover nearly the entire composition range. The data of [62Poz] and [83Ven] agree well at about 927 °C, where only ($\gamma\text{Mn,Ni}$) exists from 12.5 to 100 at.% Ni. An activity curve for (Mn) vs composition was drawn in this assessment through the concordant data of [62Poz] and [83Ven] at 927 °C, emphasizing the results of [83Ven] throughout, but—considering that the accuracy of the vapor pressure of Mn-component is greater in the 13

Section II: Phase Diagram Evaluations

Table 5 Selected Values of $-\ln\gamma_{Mn}$ in Liquid Mn-Ni Alloys at 1743 K

Composition, atom fraction Ni	$-\ln\gamma_{Mn}$					
	[75Pra]	[81Bat]	[82Jac]	[82Muk]	[85Ale]	Best fit
0.2.....	0.0	0.05	...	0.03	...	0.119
0.3.....	0.15	0.20	...	0.11	...	0.268
0.4.....	0.35	0.40	...	0.28	...	0.477
0.5.....	0.96	0.63	0.54	0.54	0.84	0.745
0.6.....	(a)	...	0.88	0.92	1.19	1.073
0.8.....	(a)	...	1.87	2.00	1.84	1.908
0.9.....	(a)	...	2.57	2.70	2.29	2.415

Note: Approximate compositional ranges of investigation in atomic percent Ni are: [75Pra], 0 to 93; [82Jac], 60 to 95; [82Muk], 10 to 90; and [85Ale], 50 to 98. (a) Out of range of best fit value, considerably smaller in γ_{Mn} than in last column.

Table 6 Thermodynamic Properties of the Liquid Mn-Ni System at 1743 K
 $xMn + (1-x)Ni = Mn_xNi_{1-x}$

Composition, atom fraction Mn	$\Delta_f G^{ex}$, J/mol	G_{Mn}^{ex} , J/mol	G_{Ni}^{ex} , J/mol	$\Delta_f H$, J/mol	H_{Mn} , J/mol	H_{Ni} , J/mol	$\Delta_f S^{ex}$, J/mol · K	S_{Mn}^{ex} , J/mol · K	S_{Ni}^{ex} , J/mol · K
0.....	0	-43 200	0	0	-56 400	0	0	-7.57	0
0.1.....	-3 890	-34 990	-430	-4 860	-41 760	-760	-0.56	-3.88	-0.19
0.2.....	-6 910	-27 650	-1 730	-8 250	-29 900	-2 840	-0.77	-1.29	-0.64
0.3.....	-9 070	-21 170	-3 890	-10 320	-20 520	-5 950	-0.72	+0.37	-1.18
0.4.....	-10 370	-15 550	-6 910	-11 210	-13 330	-9 800	-0.48	+1.27	-1.66
0.5.....	-10 800	-10 800	-10 800	-11 080	-8 050	-14 100	-0.16	+1.58	-1.89
0.6.....	-10 370	-6 910	-15 550	-10 050	-4 380	-18 560	+0.18	+1.45	-1.73
0.7.....	-9 070	-3 890	-21 170	-8 290	-2 030	-22 890	+0.45	+1.07	-0.99
0.8.....	-6 910	-1 730	-27 650	-5 930	-710	-26 800	+0.56	+0.59	+0.49
0.9.....	-3 890	-430	-34 990	-3 120	-130	-30 000	+0.44	+0.17	+2.86
1.0.....	0	0	-43 200	0	0	-32 200	0.0	0.0	+6.31

to 40 at. % Ni range—giving more weight to the results of [62Poz] in this region. The results fit the following equations for the excess partial Gibbs energies G_i^{ex} well within experimental errors:

$$G_{Mn}^{ex} = RT \ln \gamma_{Mn} = -45\,900 X_{Ni}^2 \quad \text{J/mol}$$

and

$$G_{Ni}^{ex} = RT \ln \gamma_{Ni} = -45\,900 X_{Mn}^2 \quad \text{J/mol}$$

where γ_i is the activity coefficient of i , $R = 8.3144 \text{ J/mol} \cdot \text{K}$, T is the temperature in K, and X_{Mn} and X_{Ni} are the atom fractions of Mn and Ni. The results are listed in Table 4, together with the values for the coexisting phases. In all instances, the standard state for dissolved Mn is pure β Mn, and for dissolved Ni, pure Ni at 927 °C (1200 K).

The foregoing first equation also fits the activity data for Mn from [68Ere] at 60 to 100 at. % Ni extrapolated to 777 °C (1050 K) and the data of [83Ven] at 20 to 40 at. % Ni and 777 °C, where the stable phase is (γ Mn,Ni). The results of [68Ere] for the activity of Mn are too high at 20 to 40 at. % Ni and are in large disagreement with [83Ven] and [62Poz]. The results for the phases in equilibrium with the (γ Mn,Ni) are calculated by setting the activity of Mn equal in the coexisting phases, and then calculating γ_{Mn} , from which G_{Mn}^{ex} is calculated. The results are listed in Table 4. The available data show that it is not possible to compute excess

entropies in view of the scatter in the data and relatively narrow range of temperature in these investigations.

Liquid Phase

The enthalpies of formation, *i.e.* the excess molar enthalpy H^{ex} , for the liquid alloys were investigated carefully with high-temperature calorimetry for the entire range of composition at 1500 °C by [81Bat]. The results fit a cubic Margules equation perfectly, because $H^{ex}/X_{Mn}X_{Ni}$ varies linearly with X_{Ni} ; thus:

$$H^{ex} = -X_{Mn}X_{Ni} (32\,200 + 24\,200 X_{Ni}) \quad \text{J/mol}$$

$$H_{Mn}^{ex} = -8\,000 X_{Ni}^2 - 48\,400 X_{Ni}^3 \quad \text{J/mol}$$

$$H_{Ni}^{ex} = -80\,600 X_{Mn}^2 + 48\,400 X_{Mn}^3 \quad \text{J/mol}$$

where H_i^{ex} is the excess partial enthalpy [75Gok, 86Gok]. The accuracy of the data and of these equations appears to be better than 3% at the equiatomic composition.

The activity of Mn, the more volatile component, in liquid alloys was determined first by [75Pra], using a torsion effusion cell at about 0 to 93 at. % Ni, and 1043 to 1627 °C. Dynamic flow of an inert gas directed over the liquid, transporting gaseous Mn over the alloy was used by [81Bat] in the range about 10 to 50 at. % Ni at 1300 °C to obtain the activity of Mn. The resulting data were

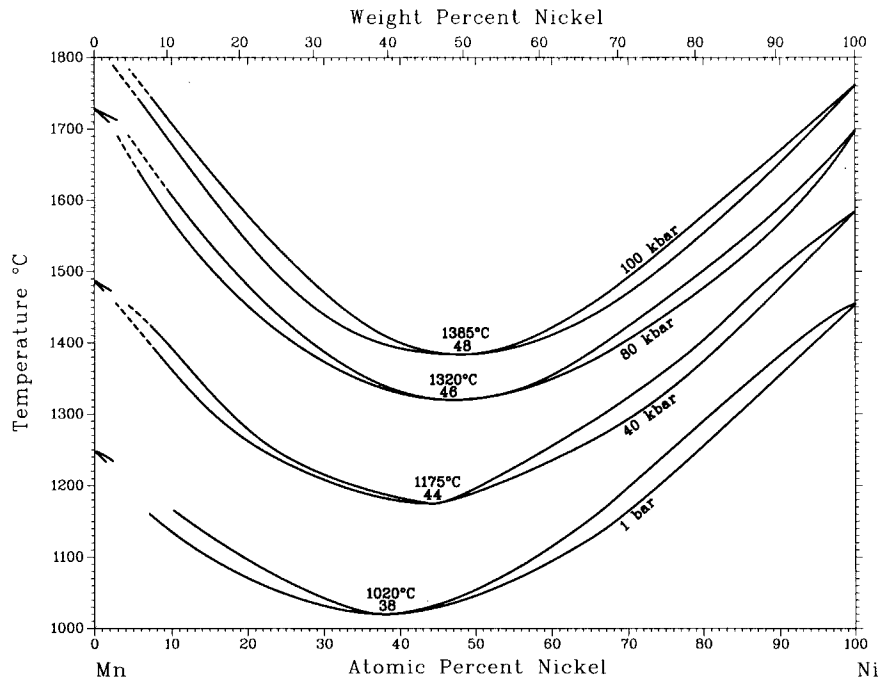


Fig. 2 Variation of Mn-Ni liquidus and solidus with pressure. From [81Ers].

considered to be tentative by [81Bat], but they appear to be in fair agreement with the subsequent data. [82Jac] determined the activity of Mn at 1410 °C from about 60 to 95 at.% Ni by using a galvanic cell with yttria-doped thoria as a solid electrolyte. [82Muk] measured the activity of Mn in the approximate range of 10 to 90 at.% Ni by an isobaric method,—Mn-Ni melt in one crucible and Fe-Mn melt in another crucible, both placed in an enclosure wherein the Mn vapor reached equilibrium over both melts at 1470 to 1620 °C. From the known activity of Mn in Fe-Mn, the activity of Mn in Mn-Ni was obtained for each alloy at each temperature. The most recent values of Mn activity were obtained by vacuum evaporation from an open surface (Langmuir method) at 1600 °C and about 50 to 68 at.% Ni [85Ale]. Selected values from [75Pra] and the values from the remaining investigations were corrected to 1743 K as necessary and then listed in Table 5. These values fit a linear relationship in $\ln \gamma_{\text{Mn}}$ vs X_{Ni}^2 , from which the following equations were derived:

$$G^{\text{ex}} = -43\,200 X_{\text{Mn}} X_{\text{Ni}} \quad \text{J/mol at 1743 K}$$

$$G^{\text{ex}}_{\text{Mn}} = RT \ln \gamma_{\text{Mn}} = -43\,200 X_{\text{Ni}}^2 \quad \text{J/mol at 1743 K}$$

$$G^{\text{ex}}_{\text{Ni}} = RT \ln \gamma_{\text{Ni}} = -43\,200 X_{\text{Mn}}^2 \quad \text{J/mol at 1743 K}$$

The results from these equations, combined with the enthalpy values, yield the excess molar entropies. Both the excess Gibbs energies and entropies are listed in Table 6 at convenient intervals. The entropy values are fairly small, and they are the least accurate properties, because a cumulative error of less than 1.3% in H^{ex} and G^{ex} would change the sign of S^{ex} at $X_{\text{Ni}} = 0.5$.

The equation for S^{ex} from $(H^{\text{ex}} - G^{\text{ex}})/(1743)$ is:

$$S^{\text{ex}} = X_{\text{Mn}} X_{\text{Ni}} (6.311 - 13.844 X_{\text{Ni}}) \quad \text{J/mol}\cdot\text{K}$$

Assuming that S^{ex} is temperature independent, G^{ex} is expressed as a function of T with the corresponding equation for $G^{\text{ex}}_{\text{Mn}}$ and $G^{\text{ex}}_{\text{Ni}}$; the results are:

$$G^{\text{ex}} = X_{\text{Mn}} X_{\text{Ni}} [-32\,200 - 6.311 T - (24\,200 - 13.884 T) X_{\text{Ni}}] \quad \text{J/mol}$$

$$G^{\text{ex}}_{\text{Mn}} = (-8\,000 - 20.195 T) X_{\text{Ni}}^2 - (48\,400 - 27.768 T) X_{\text{Ni}}^3 \quad \text{J/mol}$$

$$G^{\text{ex}}_{\text{Ni}} = (-80\,600 + 21.457 T) X_{\text{Mn}}^2 + (48\,400 - 27.768 T) X_{\text{Mn}}^3 \quad \text{J/mol}$$

These equations are in fair agreement with [75Oka] in the range of 0.3 to 0.8 atomic fraction of Mn at 1573K by touch instant emf method.

These equations may now be used to check their consistency with the corresponding equations for the solid in equilibrium with liquid and with the phase diagram. They cannot be expected to yield highly accurate results, because extrapolations to various temperatures are necessary, and errors in both sets of equations could be cumulative. The activity ratios for Mn, $a_{\text{Mn}}(\beta\text{Mn})/a_{\text{Mn}}(\text{L})$ for the solid and liquid phases, can be calculated by using the standard Gibbs energy of fusion for pure Mn, which is an estimate from [Hultgren,E]. It is reasonable to assume that the fusion equation for $\delta\text{Mn} \rightarrow \text{L}$ is close to the hypothetical fusion for $\beta\text{Mn} \rightarrow \text{L}$; thus:

Section II: Phase Diagram Evaluations

$$\Delta G^0(\beta\text{Mn} \rightarrow \text{Mn}, L) = 12\,060 - 7.939 T \\ = RT \ln a_{\text{Ni}}(\beta\text{Mn})/a_{\text{Ni}}(L) \quad \text{J/mol}$$

At 1373 K, $a_{\text{Mn}}(\beta\text{Mn})/a_{\text{Mn}}(L) = 1.11$. The phase diagram gives $X_{\text{Mn}} = 0.15$ at the solidus and $X_{\text{Mn}} = 0.20$ at the liquidus; the substitution of these equations in $G^{\text{ex}}_{\text{Mn}}$ for solid and liquid and then the computation of activities also yields 1.11 for their ratio. For the minimum point in the liquidus at 1293 K, the equation above yields 1.18, whereas the activity coefficient calculations yield 0.91.

On the Ni-rich side, the standard Gibbs energy of fusion of pure Ni is from [Hultgren,E]:

$$\Delta G^0(\text{Ni}^{\text{fcc}} \rightarrow \text{Ni}, L) = 17\,470 - 10.110 T \\ = RT \ln a_{\text{Ni}}(\gamma\text{Mn}, \text{Ni})/a_{\text{Ni}}(L) \quad \text{J/mol}$$

The liquidus and solidus at 90 to 100 at.% Ni are in accord with this equation and with [51Col] and [74Sch]. In this range, the activity ratio is very close to the atom fraction ratio. At 1473 and 1373 K, this equation gives $a_{\text{Ni}}(\gamma\text{Mn}, \text{Ni})/a_{\text{Ni}}(L) = 1.23$ and 1.37, respectively, whereas the phase diagram and the activity coefficients yield 1.16 and 1.31, respectively. For 1293 K, the preceding equation gives 1.51 and the activity coefficient computations yield 0.97 for the extrapolation of the data for $G^{\text{ex}}_{\text{Ni}}(L)$ by 470 K i.e., from 1743 to 1293 K. Thus, large errors are expected at wide extrapolations and in the more dilute regions for each component. Most of the errors seem to originate from the thermodynamic data for the solid phase, because large disagreements exist between [68Ere] and [83Ven].

Pressure

The liquid/solid Mn-Ni equilibrium diagrams at hydrostatic pressures up to 100 kbar (1 kbar = 100 MPa) were obtained by [81Ers], whose selected results are presented in Fig. 2. The minimum point composition increases from 38 to 48 at.% Ni, along with the corresponding temperature increasing from 1020 to 1385 °C. A notable aspect of the diagram is the faster increase of the melting point of pure Mn with increasing pressure than that of pure Ni.

Cited References

- 31Kay:** S. Kaya and A. Kussman, "Ferromagnetism and Phase State in Binary System Nickel-Manganese," *Z. Phys.*, **72**, 293-309 (1931) in German. (Equi Diagram; Experimental)
- *32Dou:** A. Dourdine, "On the Manganese-Nickel Alloys," *Rev. Metall.*, **29**, 507-518 and 565-573 (1932) in French. (Equi Diagram; Experimental; #)
- 40Tho:** N. Thompson, "The Order-Disorder Transformation in the Alloy Ni₃Mn," *Proc. Phys. Soc. (London)*, **52**, 217-228 (1940). (Equi Diagram; Experimental)
- 41Vol:** N. Volkenstein and A. Komar, "Coercive Force and the Magnetic Saturation of Ni₃Mn Alloy in Relation to the Order of Atomic Arrangement," *Zh. Eksp. Teor. Fiz.*, **11**, 723-724 (1941) in Russian. (Equi Diagram; Experimental)
- *48Kos:** W. Koster and W. Rauscher, "Contribution to Nickel-Manganese System," *Z. Metall.*, **39**, 178-184 (1948) in German. (Equi Diagram, Crys Structure; Experimental; #)
- 49Kur:** N.N. Kurnakov and M.Y. Troneva, "The System Manganese-Nickel," *Dokl. Akad. Nauk SSSR*, **68**, 73-76 (1949) in Russian. (Equi Diagram; Experimental; #)
- 49Shu:** G.C. Shull and S. Siegel, "Neutron Diffraction Studies of Order-Disorder in Alloys," *Phys. Rev.*, **75**, 1008-1010 (1949). (Crys Structure; Experimental)
- *51Col:** B.R. Coles and W. Hume-Rothery, "The Equilibrium Diagram of the System Nickel-Manganese," *J. Inst. Met. (London)*, **80**, 85-92 (1951-52). (Equi Diagram, Crys Structure, Thermo; Experimental; #)
- *52Ere1:** V.N. Eremenko and V.I. Skuratovskaya, "The Effect of Addition of Nickel on Polymorphic Changes of Manganese," *Ukr. Khim. Zh.*, **18**, 213-218 (1952) in Russian. (Equi Diagram; Experimental; #)
- *52Ere2:** V.N. Eremenko and T.D. Shtepa, "The Equilibrium Diagram of the System Manganese-Nickel," *Ukr. Khim. Zh.*, **18**, 219-231 (1952) in Russian. (Equi Diagram; Experimental; #)
- 55Shu:** G.C. Shull and M.K. Wilkinson, "Neutron Diffraction Studies of the Magnetic Structure of Alloys of Transition Elements," *Phys. Rev.*, **97**, 304-310 (1955). (Equi Diagram, Crys Structure; Experimental)
- *57Hel:** A. Hellawell and W. Hume-Rothery, "The Constitution of Alloys of Iron and Manganese with Transition Elements of the First Long Period," *Philos. Trans. R. Soc., (London) A*, **249**, 417-459 (1957). (Equi Diagram; Experimental; #)
- 57Pea:** W.B. Pearson and L.T. Thompson, "The Lattice Spacings of Nickel Solid Solutions," *Can. J. Phys.*, **35**, 349-357 (1957). (Crys Structure; Experimental)
- 58Hah:** R. Hahn and E. Kneller, "Magnetic Properties and Order Structure of Nickel-Manganese Alloys. I. Quasi Paramagnetism of Partially Ordered Nickel-Manganese Alloys," *Z. Metallkd.*, **49**, 426-441 (1958) in German. (Equi Diagram; Experimental)
- 59Kas:** J.S. Kasper and J.S. Kouvel, "The Magnetic Structure of NiMn," *J. Phys. Chem. Solids*, **11**, 231-238 (1959). (Equi Diagram, Crys Structure; Experimental)
- 61Mar:** M.J. Marcinkowski and N. Brown, "Transformation Disorder-to-Order in Ni₃Mn," *J. Appl. Phys.*, **32**, 375-386 (1961). (Equi Diagram, Crys Structure; Experimental)
- *62Poz:** G.V. Pozharskaya and A.M. Evseev, "Thermodynamics of Manganese-Nickel Alloys," *Russ. J. Phys. Chem.*, **36**, 726 (1962) in English. (Thermo; Experimental)
- 63Kro:** R.S. Krogstad, R.W. Moss, and V. Vali, "Note Concerning the Mossbauer Study of the Order-Disorder Transformation in Ni₃Mn," *Phys. Lett.*, **4**, 44-45 (1963). (Equi Diagram, Crys Structure; Experimental)
- 65Pat:** W.R. Patterson, "The fcc → fct Gamma Manganese Transformation in Mn-Ni Alloys," *Trans. Metall. Soc. AIME*, **223**, 438-440 (1965). (Meta Phases, Crys Structure; Experimental)
- 65Pea:** W.B. Pearson, K. Brun, and A. Kjekshus, "Equiatomic Transition Metal Alloys of Manganese III. The Tetragonal NiMn Phase," *Acta Chem. Scand.*, **19**, 477-484 (1965). (Crys Structure; Experimental)
- 66Pao:** A. Paoletti, F.P. Ricci, and L. Passari, "Magnetization and State of Order in MnNi₃," *J. Appl. Phys.*, **37**, 3236-3239 (1966). (Crys Structure; Experimental)
- 67Kra:** V. Krasevec, P. Delavignette, and S. Amelinckx, "Superstructure Due to Periodic Twinning in Quenched NiMn-Alloy," *Mater. Res. Bull.*, **2**, 1029-1034 (1967). (Meta Phases; Experimental)
- 67Pao:** A. Paoletti and F.P. Ricci, "Coexisting Phases in Partially Ordered MnNi₃," *Phys. Lett. A*, **24**, 371-372 (1967). (Crys Structure; Experimental)
- *68Ere:** V.N. Eremenko, G.M. Lukashenko, and V.R. Sidorko, "Thermodynamic Properties of Nickel-Manganese System Alloys," *Izv. Akad. Nauk, SSSR, Met.*, (2), 208-214 (1968) in Russian. (Thermo; Experimental)
- 68Hic:** T.J. Hicks, A.R. Pepper, and J.H. Smith, "Antiferromagnetism in Gamma-Phase Manganese-Palladium and Manganese-Nickel Alloys," *J. Phys. C (London), Series 2*, **1**, 1683-1689 (1968). (Equi Diagram; Experimental)

- *68Kre: E. Kren, E. Nagy, I. Nagy, L. Pal, and P. Szabo, "Structures and Phase Transformations in the Mn-Ni System Near Equiatomic Concentration," *J. Phys. Chem. Solids*, 29, 101-108 (1968). (Equi Diagram, Crys Structure; Experimental)
- 68Pal: L. Pal, E. Kren, G. Kadar, P. Szabo, and T. Tarnoczi, "Magnetic Structures and Phase Transformations in Mn-Based CuAu-I Type Alloys," *J. Appl. Phys.*, 39, 538-544 (1968). (Equi Diagram, Crys Structure; Experimental)
- *69Tsi: K.E. Tsiuplakis and E. Kneller, "Manganese-Nickel Phase Diagram," *Z. Metallkd.*, 60, 433-438 (1969) in German. (Equi Diagram, Crys Structure; Experimental; #)
- 74Bee: J.C. Beers II and L. Guttman, "Thermodynamic Character of the Order-Disorder Transition in Nickel-Manganese Alloys," *Phys. Rev. B, Solid State*, 9, 3941-3943 (1974). (Equi Diagram; Experimental)
- 74Sch: E. Schurmann and B. Prinz, "Equilibria in Fusion of Ni-Rich and Cu-Rich Cu-Mn-Ni Alloys, II," *Z. Metallkd.*, 65, 593-596 (1974). (Thermo; Experimental)
- 75Gok: N.A. Gokcen, *Thermodynamics*, Techscience Inc., Hawthorne, CA (1975). (Thermo; Theory)
- 75Oka: K. Okajima and H. Sakao, "Activity Measurements of the Binary Mn-Base Molten Alloys by the TIE Method," *Trans. Japan Inst. Metals*, 16(2), 87-93 (1975). (Thermo; Experimental)
- *75Pra: J.N. Pratt and N. Ahmad, "Thermodynamics of Alloys. Vapor Pressure Studies of Manganese-Nickel and Manganese-Silicon Liquid Alloys," U.S. NTIS, Rep. Ad-A017668, 38 p (1975). (Thermo; Experimental)
- 77Koz: E.V. Kozlov and A.S. Taylashev "Order-Disorder Transformation in the Stoichiometric Alloy Ni₃Mn," *Fiz. Met. Metalloved.*, 43, 610-614 (1977) in Russian. (Equi Diagram, Crys Structure; Experimental)
- *81Bat: G.I. Batalin, V.A. Stukalo, N.Y. Neshchimenko, and N.V. Patse-ly, "Thermodynamic Properties of Binary Mn-Ni Melts," *Z. Fiz. Khim.*, 55, 2469-2471 (1981) in Russian. (Thermo; Experimental)
- *81Ers: T.P. Ershova, N.D. Fradkova, and Y.A. Litvin, "Construction of the T-P-N Fusibility Diagram for the Mn-Ni System for Pressures up to 100 kbar," *Metalli*, (5), 192-197 (1981) in Russian. (Pressure; Experimental; #)
- *81Ogd: N.F. Ogdansky and V.G. Otroschenko, "The Structure of Rapidly Crystallized Manganese-Nickel Alloys," *Fiz. Met. Metalloved.*, 51, 1099-1101 (1981) in Russian. (Meta Phases; Experimental)
- *82Jac: K.T. Jacob, "Activity of Manganese in Liquid Ni-Mn Alloys," *Metall. Trans. B*, 13, 283-285 (1982). (Thermo, Experimental)
- *82Muk: K. Mukai, Y. Wasai, K. Funatsu, K. Wasai, and H. Koda, "Measurements of the Activity of Manganese in Molten Nickel-Manganese Alloys by an Isobaric Method," *J. Jpn. Inst. Met.*, 46, 870-877 (1982) in Japanese. (Thermo; Experimental)
- 83Ego: V.E. Egorushkin, S.N. Kulkov, and S.E. Kulkova, "Investigation on Phase Transitions in NiMn," *Sov. Phys. JETP*, 57(2), 345-349 (1983). (Equi Diagram; Experimental)
- *83Ven: M. Venkataraman and J.P. Hajra, "Thermodynamics of Nickel-Manganese Alloys Using Oxide and Fluoride Electrolytes," *Metall. Trans. A*, 14, 2125-2130 (1983). (Thermo; Experimental)
- *85Ada: K. Adachi and C.M. Wayman, "Transformation Behavior of Nearly Stoichiometric Ni-Mn Alloys," *Metall. Trans. A*, 16, 1567-1579 and 1581-1597 (1985). (Meta Phases, Crys Structure; Experimental)
- *85Ale: R.A. Aleev, V.K. Bakanov, Y.V. Balkovoi, V.A. Grigoryan, M.A. Golub, and B. Rakutuvelu, "Determination of the Activity of Manganese in Molten Nickel by Evaporation from an Open Surface," *Izv. V. U. Z., Chernaya Metall.*, (9), 20-24 (1985) in Russian. (Thermo; Experimental)
- 86Gok: N.A. Gokcen, *Statistical Thermodynamics of Alloys*, Plenum Press, New York (1986). (Thermo; Compilation)
- 86Gup: K.P. Gupta, S.B. Rajendraprasad, A.K. Jena, and R.C. Sharma, "The Copper-Manganese-Nickel-System," *J. Alloy Phase Diagrams (India)*, 2, 198-204 (1986). (Equi Diagram; Review)
- 89Gok: N.A. Gokcen, "The Phase Transformations in Mn," *Bull. Alloy Phase Diagrams*, 10, 313 (1989). (Thermo; Review)
- 90Gok: N.A. Gokcen, "The Mn-N (Manganese-Nitrogen) System," *Bull. Alloy Phase Diagrams*, 11, 33-42 (1990). (Crys Structure; Review)

Mn-Ni evaluation contributed by N.A. Gokcen, 440 East Thornton Lake Dr., Albany, OR 97321. This work was supported by ASM International. Dr. Gokcen is the Alloy Phase Diagram Program Category Editor for binary manganese alloys.

The Ag-Th (Silver-Thorium) System

By M.R. Baren
Temple University

Equilibrium Diagram

[43Rau] investigated the Ag-Th equilibrium diagram for alloy compositions between 0 and 64.6 at.% Th using thermal, X-ray, and metallographic analyses and resistance-capacitance tests. Alloys were prepared by melting powder compacts in either clay or sintered alumina crucibles. Clay crucibles were used for low-Th concentrations while alumina crucibles were used for Th-rich alloys. For the Th-rich alloys, it was difficult to inhibit the formation of thorium oxides. Consequently, compositions were reported

after adjusting for contamination by ThO₂, and the results for compositions greater than 40 at.% Th are uncertain. The assessed Ag-Th phase diagram (Fig. 1) is characterized by three intermediate phases that form congruently from the melt. [43Rau] reported the two Ag-rich compounds to be Ag₃Th and "Ag₅Th₃." However, the X-ray and density measurements of arc-melted stoichiometric Ag₂Th by [61Bro] showed that the compound "Ag₅Th₃" [43Rau] is actually Ag₂Th. In addition, it is likely that Ag₃Th is actually Ag_{3,6}Th and isostructural with Ag_{3,6}Gd which structure was determined by [71Bai].